Effects of Nano Calcium Carbonate Modified by a Lanthanum Compound on the Properties of Polypropylene

Tao Guo,[1] Lianshi Wang,[1] Anqiang Zhang,[1] Tongmin Cai[2]

[1]*Key Laboratory of Polymer Processing Engineering of the Ministry of Education, College of Material Science and Engineering, South China University of Technology, 510640, Guangzhou, People's Republic of China*
[2]*Guangzhou Kingfa Science and Technology Company, Limited, 510520, Guangzhou, People's Republic of China*

ABSTRACT: The surface modification of nano calcium carbonate ($nCaCO_3$) particles was carried out with a soluble compound of lanthanum via a coating process of chemical deposition, and $nCaCO_3$ particles covered with a compound of lanthanum ($nCaCO_3$–La) were prepared. The polypropylene (PP)/$nCaCO_3$ and PP/$nCaCO_3$–La composites were prepared with a two-roll mill. The measurements of the mechanical properties showed that the impact strength of the composites increased at first and then decreased with the addition of fillers, and the tensile strength was reduced at the same time. The impact strength of PP/$nCaCO_3$–La was higher than that of PP/$nCaCO_3$, and the impact strength of PP/$nCaCO_3$–5La was three times that of virgin PP. Transmission electron microscopy and scanning electron microscopy showed that $nCaCO_3$–La dispersed well in the PP matrix, the size distribution of the particles was uniform, and $nCaCO_3$–La adhered to the PP matrix very closely. The crystallization properties of virgin PP and its composites were studied with differential scanning calorimetry and wide-angle X-ray diffraction. The results showed that the β-PP phase easily formed with the addition of the lanthanum compound. In comparison with virgin PP, the addition of $nCaCO_3$–La led to a higher crystallization temperature. The size of the crystallites increased with the addition of $nCaCO_3$–La, and the nucleation of PP crystalline was also improved. © 2005 Wiley Periodicals, Inc. J Appl Polym Sci 97: 1154–1160, 2005

Key words: crystallization; mechanical properties; poly(propylene) (PP)

INTRODUCTION

Among the different methods used to toughen polypropylene (PP), the addition of rubber has been the most successful and conventional.[1] However, its most obvious shortcoming for PP is the reduction of the stiffness and heat resistance. For this reason, inorganic fillers are used to improve the modulus of the matrix, and nano calcium carbonate ($nCaCO_3$) is one of the most widely used fillers for modifying PP.[2,3] However, $nCaCO_3$ particles have high surface free energy and tend to aggregate. To reduce the strong surface free energy, the surface of $nCaCO_3$ should be modified. As $nCaCO_3$ does not exhibit good adhesion and dispersion in a matrix of PP, various surface treatments have been applied.[4,5] Much research has been reported about the surface modification of $nCaCO_3$[6,7] and the effects of modified $nCaCO_3$ on the properties of PP.[8] The most widely used methods of surface modification are surface grafting and coupling, such as the grafting of unsaturated carboxylic acids and the coupling of titanates, aluminates, phosphates, and zirconates.[9–12] The coating process of chemical deposition is a new method for modifying the surface of inorganic particles.[13] However, there has been no study so far on the modification of $nCaCO_3$ particles covered with rare earth (RE) compounds by the method of chemical deposition.

RE compounds have special electronic structures, and polymer modification by REs is a new field of research.[14] Some research has shown that REs have a very strong inductive effect on polymers,[15,16] and some properties of polymers are enhanced by the addition of REs.[17] Unlike other modifiers, REs can improve polymer properties in small amounts.

Feng et al.[17] used a complex of trivalent lanthanum stearate with stearin as a surface modifier to treat $nCaCO_3$ by mechanical mixing, and its efficacy was assessed. They found that the surface properties of $nCaCO_3$ could be changed. In our research, we used $nCaCO_3$ particles as a support and covered the lanthanum compounds on the particle surface through chemical deposition. This method not only makes good use of the special properties of RE but also saves RE resources. In this work, we mainly developed a study of the mechanical and crystalline properties of PP/$nCaCO_3$–La composites.

Correspondence to: T. Guo (phoebe_ho@tom.com).

EXPERIMENTAL

Materials and process of deposition

The nCaCO$_3$ used in this study came from Guangping Chemical Corp. (Guangdong, China). The average particle size was 40 nm. The lanthanum compound (99.9%) came from Zhujiang Chemical Factory (Guangzhou, China). First, the soluble lanthanum compound was dissolved in distilled water, and then it was dropped into an nCaCO$_3$ suspension at room temperature. The precipitant of the alkali solution was also dropped into the mixing system. After the deposition was finished, the resulting precipitate was filtered, washed, and dried at 70–80°C *in vacuo* until a steady weight was obtained, and nCaCO$_3$ particles modified with a lanthanum compound (nCaCO$_3$–La) were obtained; the compound was nCaCO$_3$ covered with La(OH)$_3$. The PP (F401) came from Guangzhou Petrochemical Factory (Guangzhou, China), and its melt flow rate was 3.0 g/10 min.

Preparation and characterization of the PP/nCaCO$_3$–La composites

PP was dried in an oven at 80°C for 4 h and then was melted and blended with different filler concentrations with a laboratory two-roll mill at 170–175°C for 10 min; this was followed by compression molding at 185°C. There were three composites, PP/nCaCO$_3$, PP/nCaCO$_3$–1La, and PP/nCaCO$_3$–5La, in this experiment, and the La$_2$O$_3$ concentrations were 0, 1, and 5 phr, respectively. The PP concentration was 100 phr. The specimens were cut from 4-mm-thick sheets for the testing of the mechanical properties. The notched Izod impact strength was measured at 25°C according to GB1843-96 with a impact tester. The tensile strength was measured on a Shimadzu AG1 (Kyoto, Japan) mechanical tester according to GB1040-92.

The fresh impact-fracture surfaces were sputtered with gold and observed under a Philips XL30 FEG (Best, The Netherlands) scanning electron microscope. Ultrathin sections of compression-molded specimens were prepared with an LKB Ultrotome V (Tokyo, Japan) ultramicrotome. The electron micrographs were obtained with a JEM 100-CXII (Tokyo, Japan) transmission electron microscope.

Differential scanning calorimetry (DSC) measurements were carried out on a PerkinElmer Pyris (Wellesley, MA) differential scanning calorimeter. The sample was heated from 25 to 250°C quickly, maintained there for 10 min for the elimination of the thermal history, cooled to 25°C at a rate of 10°C/min, and reheated from 25 to 250°C at the same rate. The temperature and heat capacity scales were calibrated from the melting scans of high-purity indium and zinc samples at the same heating rate.
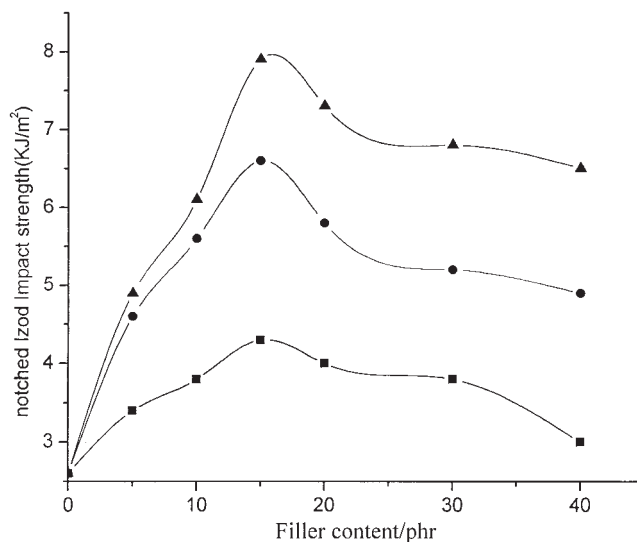
Figure 1 Effects of the filler content on the impact strength: (■) nCaCO$_3$, (●) nCaCO$_3$–1La, and (▲) nCaCO$_3$–5La.

Wide-angle X-ray diffraction (WAXD) was carried out on a wide-angle D-MAX/1200 (Bruker Company, Rheinstetten, Germany) vertical goniometer used to measure the amount of crystallinity in the composites. The applied radiation was Cu Kα from a long fine-focus Cu tube.

RESULTS AND DISCUSSION

Mechanical properties
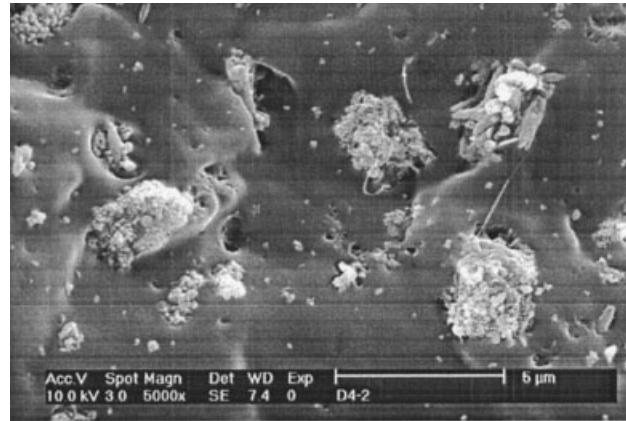
Figure 1 presents the effects of the nCaCO$_3$, nCaCO$_3$–1La, and nCaCO$_3$–5La concentrations on the notched Izod impact strength of PP/nCaCO$_3$, PP/nCaCO$_3$–1La, and PP/nCaCO$_3$–5La, respectively. With an increase in the filler concentration, the notched Izod impact strengths of all three composites increased and then decreased. The maximum impact strength was achieved at a loading of approximately 15 phr. According to the trend of the impact strength variation, the PP/nCaCO$_3$–La composite increased more obviously than PP/nCaCO$_3$. When the concentration of untreated nCaCO$_3$ was 40 phr, the impact strength had already decreased to the level of virgin PP, and the maximum impact strength of PP/nCaCO$_3$ was 4.3 kJ/m^2. By contrast, the maximum impact strengths of PP/nCaCO$_3$–5La and PP/nCaCO$_3$–1La were 7.9 and 6.6 kJ/m^2, about 300 and 250% of that of virgin PP, respectively, and the two composites maintained a high level of impact strength when the concentration increased to 40 phr. As expected, in contrast with nCaCO$_3$, the nCaCO$_3$ treated with the lanthanum compound had a more obvious toughening effect on PP. The lanthanum compound that covered nCaCO$_3$, therefore, had a special modification ability to improve the impact strength of PP.
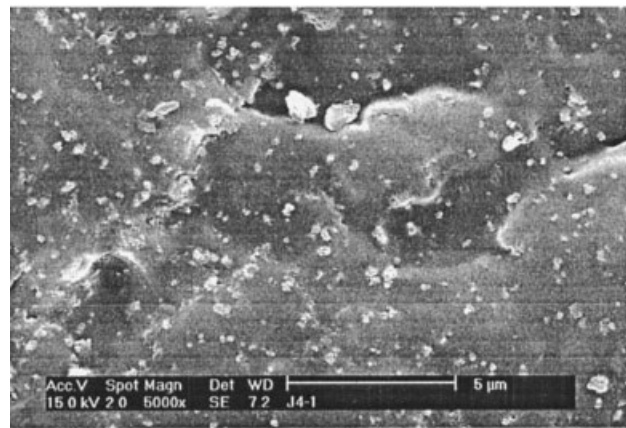
As similarly found in other studies,[18,19] the tensile strengths of all three composites decreased with an increasing filler loading, and they leveled when the loading was close to 30 phr, but the tensile strengths of both PP/nCaCO$_3$–5La and PP/nCaCO$_3$–1La were higher than that of PP/nCaCO$_3$, as shown in Figure 2. With a low filler loading (0–10 phr), unlike that of PP/nCaCO$_3$, the tensile strength of PP/nCaCO$_3$–5La maintained a high level and decreased slowly when the loading of nCaCO$_3$–5La was more than 30 phr. Altogether, the mechanical properties of the three composites were as follows: PP/nCaCO$_3$–5La > PP/nCaCO$_3$–1La > PP/nCaCO$_3$. For PP/nCaCO$_3$–5La, a composite with good mechanical properties could be achieved when the filler loading was changed from 10 to 20 phr.
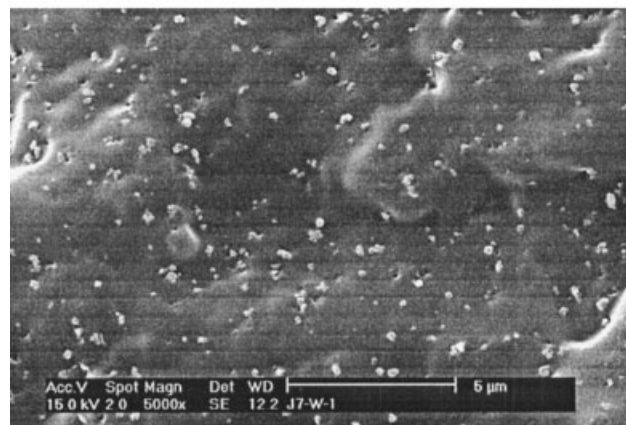
Analysis by microphotographs

Figure 3(a–c) illustrates the morphology of the impact-fracture surface of three composites with 10 phr filler. Figure 3(a) is a photograph of the impact-fracture surface of the PP/nCaCO$_3$ sample. The particles of nCaCO$_3$ were dispersed in the matrix of PP irregularly, and some big aggregates were exposed on the fracture surface, with a particle size greater than 2 μm. By observing these aggregations, we found that they were formed of many primary particles. The PP/nCaCO$_3$ sample had a large particle size of 2–4 μm. From an analysis of the mechanical properties, we determined that this composite exhibited an impact energy only slightly higher than that of virgin PP and much lower than that of the PP/nCaCO$_3$–5La composites. Figure 3(b,c) presents photographs of the impact-fracture surface of PP/nCaCO$_3$–1La and PP/nCaCO$_3$–

(a)

(b)

(c)

Figure 3 Scanning electron micrographs of composites (100/10): (a) PP/nCaCO$_3$, (b) PP/nCaCO$_3$–1La, and (c) PP/nCaCO$_3$–5La.
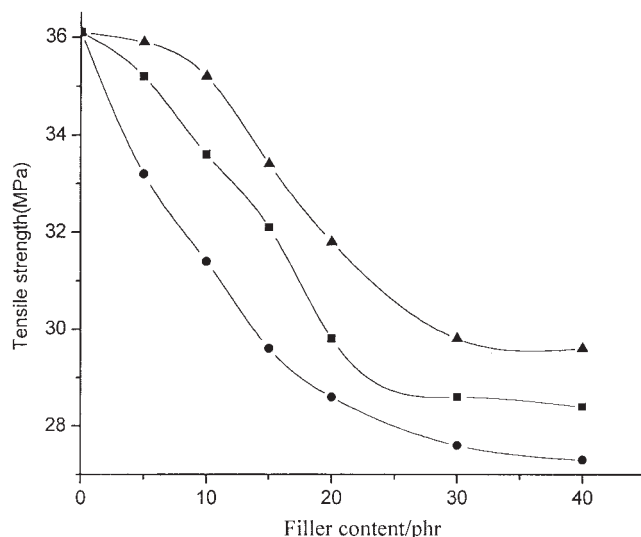
Figure 2 Effects of the filler content on the tensile strength: (■) nCaCO$_3$, (●) nCaCO$_3$–1La, and (▲) nCaCO$_3$–5La.

5La composites. In PP/nCaCO$_3$–1La, there were no aggregates, and the average particle size was smaller than that of nCaCO$_3$. When the amount of the lantha-
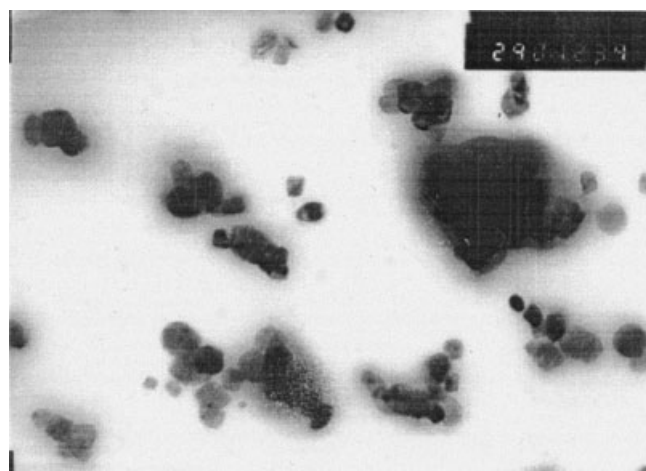
(a)
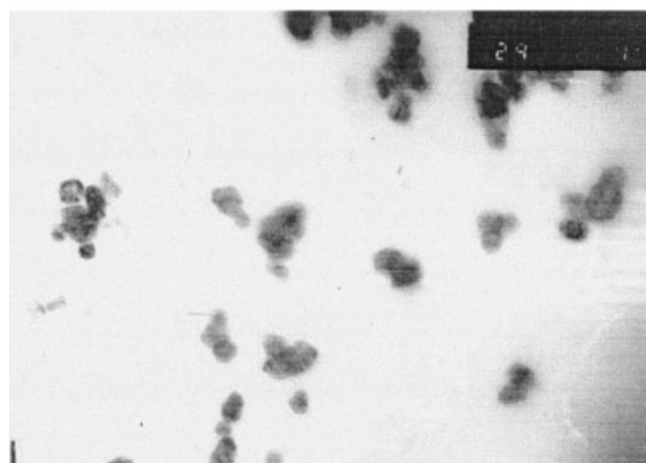
(b)

Figure 4 Transmission electron micrographs of composites (100/10): (a) PP/nCaCO$_3$ and (b) PP/nCaCO$_3$–5La.

num compound covering the nCaCO$_3$ particles increased, the dispersion of the nCaCO$_3$–5La particles in the PP matrix became more uniform, as Figure 3(c) demonstrates. Most nCaCO$_3$–5La particles were under 100 nm, and the combination of nCaCO$_3$–5La particles with the PP matrix was very close; this was the main reason for the high toughness.

Figure 4(a,b) shows transmission electron micrographs of ultrathin sections of PP/nCaCO$_3$ and PP/nCaCO$_3$–5La with a filler concentration of 10 phr. The impact property of the nCaCO$_3$-filled specimen was compromised by the aggregation of the nCaCO$_3$ particles, as shown in Figure 4(a); many aggregates were

present in the matrix. The large aggregate of nCaCO$_3$ particles was more than 0.8 μm, and the small one was no less than 100 nm; the number of primary particles was very low. The aggregates provided a convenient trigger for brittle behavior because of their large sizes and sharp edges; the data for the mechanical properties are shown in Figures 1 and 2. In contrast, nCaCO$_3$–5La showed much fewer aggregates than nCaCO$_3$, as shown in Figure 4(b). Although there were some aggregates, the number was very low, and the nCaCO$_3$–5La particles dispersed in PP were 40–100 nm.

Earlier research has shown that only ultrafine inorganic particles can toughen plastics.[20] The nCaCO$_3$ used in this work was a nanofiller, but when blended with PP without a surface treatment, it tended to aggregate and could not disperse on a nanoscale. The reason for this was that the surface energy of nCaCO$_3$ was very high and the polarity of nCaCO$_3$ differed from that of PP, so it could not be used as a toughening agent. When the surface of nCaCO$_3$ was covered with a layer of the lanthanum compound, it could disperse uniformly in the PP matrix for the nanoparticles, aggregation could be avoided, and the adhesion between the filler and resin was enhanced by the effect of the lanthanum compound. Therefore, the mechanical properties, especially the impact strength of the composites, were effectively improved.

Thermal analysis by DSC

The influence of the nCaCO$_3$–La fillers on the crystallization of PP was studied with DSC, and this study included nonisothermal crystallization and melting behavior. Figure 5(a) shows the DSC cooling curves obtained for virgin PP, PP/nCaCO$_3$, PP/nCaCO$_3$–1La, and PP/nCaCO$_3$–5La. In comparison with that of virgin PP, the crystal peak of the composites moved to a high temperature, and the movement of PP/nCaCO$_3$–5La was the most obvious. As shown in Figure 5(b), there were almost no differences in the melting behavior between virgin PP and the composites. Table I presents the DSC data for nonisothermal crystallization and melting. T_{co}, T_{cp}, T_{cf}, and T_{mp} are the onset temperature of crystallization, the peak temperature of crystallization, the finished temperature of crystallization, and the peak temperature of melting, respectively; ΔH_m is the heat of melting of PP; and X_c is the value of the crystallinity.

The data in Table I show that the nCaCO$_3$–1La and nCaCO$_3$–5La fillers had some influence on the nucleation of PP crystallites, increasing the crystallization temperature by more than 6 and 8°C, respectively; this demonstrated an obvious influence on the kinetics of crystallization of PP. However, nCaCO$_3$ induced only a very slight increase in the crystallization temperature (T_{cp}) in the range of 1.7°C. ΔT ($T_{mp} - T_{cp}$) is an

(a)

(b)
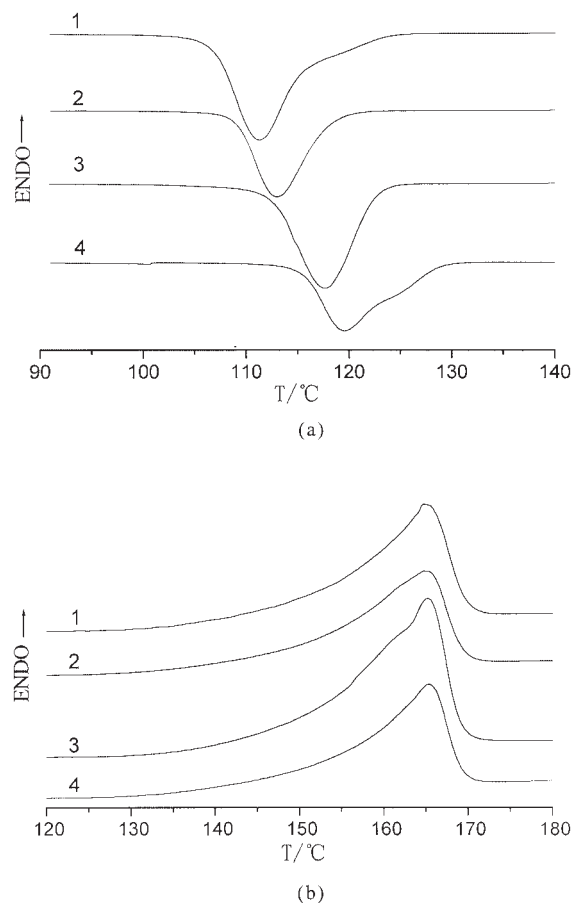
Figure 5 (a) Crystallization and (b) melting DSC crystalline curves of virgin PP and composites: (1) virgin PP, (2) PP/nCaCO$_3$ (100/10), (3) PP/nCaCO$_3$–1La (100/10), and (4) PP/nCaCO$_3$–5La (100/10).

index representing the crystallization ratio; ΔT of PP/nCaCO$_3$–La was lower than ΔT of PP/nCaCO$_3$ and virgin PP, as shown in Table I. This demonstrated that the crystallization ratio of PP/nCaCO$_3$–La was higher than that of PP/nCaCO$_3$ and virgin PP. The difference between PP/nCaCO$_3$–1La, PP/nCaCO$_3$–5La, and virgin PP can also be seen in the degree of crystallinity. The degree of crystallinity of PP/nCaCO$_3$–1La and PP/nCaCO$_3$–5La decreased by up to 2.1 and 0.5%, respectively.

To learn about the effects of the nCaCO$_3$–5La concentrations on the crystalline properties, difference curves were constructed from the cooling curves of
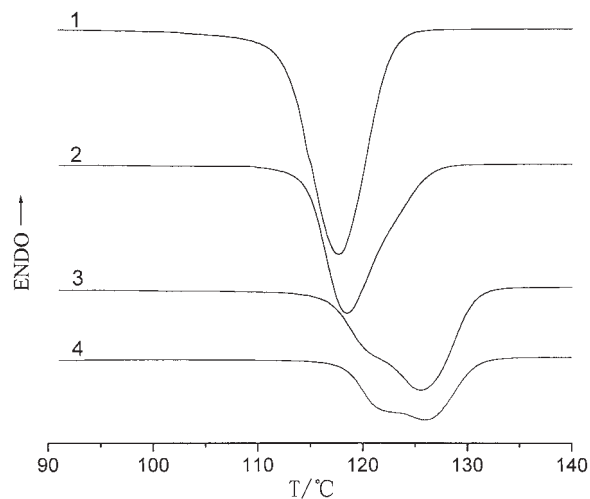
Figure 6 DSC crystalline curves of PP/nCaCO$_3$–5La with different filler contents: (1) 5, (2) 10, (3) 15, and (4) 20 phr.

PP/nCaCO$_3$–5La composites, and they are presented in Figure 6. These curves imply that the crystallization temperature increased with an increasing concentration of nCaCO$_3$–5La. Table II presents the data for the nonisothermal crystallization. The data demonstrate that the concentration of the nCaCO$_3$–5La fillers had some influence on PP crystallites; the crystallization temperature increased by 4.3, 6.2, 12.2, and 13.0°C when the concentration was 5, 10, 15, and 20 phr, respectively. Additionally, the degree of crystallinity of PP was reduced by the addition of the nCaCO$_3$–5La filler. The minimum X_c value of PP/nCaCO$_3$–5La was achieved with a loading of 20 phr; it was 39.9%.

From the DSC data, we concluded that the presence of nCaCO$_3$–1La and nCaCO$_3$–5La markedly influenced the crystallization behavior of PP; after the surface of nCaCO$_3$ particles was covered with the lanthanum compound, the nucleating ability of PP was improved by the addition of the fillers.

WAXD measurements

Figure 7 shows WAXD patterns of virgin PP and three composites. For virgin PP, as shown in curve 1, there were five peaks of diffraction at diffraction angles (2θ) of 14.3, 17.0, 18.6, 21.4, and 22.0°, which corresponded to crystal planes of (110), (040), (130), (111), and (131),

TABLE I
DSC Crystalline Parameters of Pure PP and Composites

Sample	T_{co} (°C)	T_{cp} (°C)	T_{cf} (°C)	ΔH_m (J/g)	T_{mp} (°C)	$T_m - T_c$ (°C)	X_c (%)
Virgin PP	125.2	111.3	102.7	94.6	165.7	54.4	45.3
PP/nCaCO$_3$ (100/10)	122.6	113.0	106.3	86.8	165.6	52.6	41.5
PP/nCaCO$_3$–1La (100/10)	126.2	117.8	108.4	90.2	165.2	47.4	43.2
PP/nCaCO$_3$–5La (100/10)	130.8	119.5	112.3	93.7	165.5	46.0	44.8

TABLE II
**DSC Crystalline Parameters of PP/nCaCO$_3$-5La with Different Filler Contents**

Sample	ΔH_c (J/g)	X_c (%)	T_{co} (°C)
Virgin PP	94.6	45.3	113.3
PP/nCaCO$_3$–5La (100/5)	93.8	44.9	117.6
PP/nCaCO$_3$–5La (100/10)	93.7	44.8	119.5
PP/nCaCO$_3$–5La (100/15)	88.7	42.4	125.5
PP/nCaCO$_3$–5La (100/20)	83.4	39.9	126.3

TABLE III
WAXD Data of PP and Its Composites

Sample	Crystal plane	2θ (°)	d (nm)	l (%)	$B_{1/2}$ (°)
Virgin PP	110	14.5	0.62	100	0.842
	040	17.0	0.52	62.6	0.947
	130	18.6	0.47	48.9	1.368
PP/nCaCO$_3$ (100/10)	110	14.3	0.62	100	0.663
	040	17.0	0.52	60.8	0.789
	130	18.6	0.47	50.9	1.316
PP/nCaCO$_3$–1La (100/10)	110	14.2	0.62	73.1	0.737
	040	17.0	0.52	100	0.632
	130	18.6	0.48	60.1	0.947
	300	15.7	0.56	47.1	0.438
PP/nCaCO$_3$–5La (100/10)	110	14.3	0.62	95.1	0.737
	040	17.0	0.52	100	0.653
	130	18.6	0.48	58.7	1.368
	300	16.1	0.55	69.5	0.564

respectively. It was the typical crystal form of α-PP. Data from WAXD curves for the four samples are listed in Table III; d is the crystal plane distance, I is the relative intensity of the peak, and $B_{1/2}$ is the half-height width of the crystallization peak.

In comparison with virgin PP, a new diffraction peak appeared in the curve of PP/nCaCO$_3$–1La and PP/nCaCO$_3$–5La, and it lay at $2\theta = 16°$. It was a typical β spherulite of PP. The relative amount of the β phase (f_β) was determined with the following relation:[21]

$$f_\beta = I_\beta / (I_{\alpha1} + I_{\alpha2} + I_{\alpha3} + I_\beta)$$

where I_β is the intensity of the peak for the (300) diffraction plane of the β phase, and I_α is the intensity of the peak for the (110), (040), or (030) diffraction plane of the α phase. The f_β values of the samples are listed in Table IV. Only PP/nCaCO$_3$–1La and PP/nCaCO$_3$–5La had f_β values, and they were 16.8 and 21.5%, respectively. As shown by the diffraction curve, the intensity of the peak for the (300) diffraction plane of PP/nCaCO$_3$–5La was stronger than that for PP/nCaCO$_3$–1La. Thus, the incorporation of nCaCO$_3$–1La and nCaCO$_3$–5La into the PP matrix generally led to an increase in the relative content of the β form.
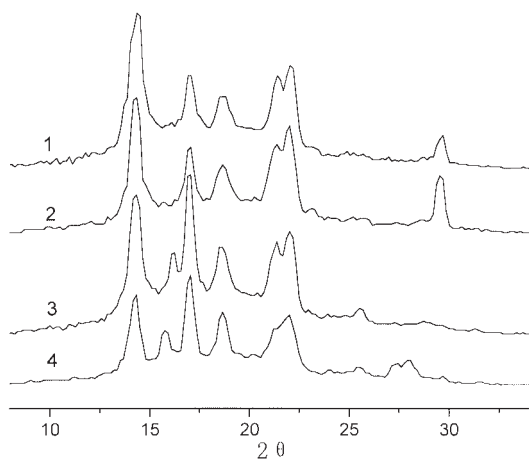
Figure 7 WAXD patterns of PP and composites: (1) virgin PP, (2) PP/nCaCO$_3$ (100/10), (3) PP/nCaCO$_3$–1La (100/10), and (4) PP/nCaCO$_3$–5La (100/10).

Because f_β of PP/nCaCO$_3$ was zero, we could draw the conclusion that the lanthanum compound could initiate the β-phase crystallinity of PP. It is well known that there are α, β, γ, and δ crystal forms in PP.[22] The α spherulite is the main crystal form, and the β spherulite and others are formed only on some special occasions.[23] According to the research of Tjong et al.,[24,25] β-PP has greater toughness than α-PP. Therefore, this is the other main reason for the toughening effect of nCaCO$_3$–La, and this is consistent with the analysis from Figure 1.

The size of the crystallites (L_{hkl}) was determined with the Scherrer relation:[26]

$$L_{hkl} = K\lambda / B_{1/2}\theta$$

where $\lambda = 0.1541$ nm is the X-ray wavelength and $K = 0.89$ is the coefficient. The L_{hkl} values of the samples are listed in Table IV. Compared with that of PP, the L_{hkl} values of the composites increased with the addition of fillers. Therefore, the fillers could improve nucleation.

X_c can be represented as follows:

$$X_c = \Sigma S_c / \Sigma S$$

where ΣS_c is the crystal diffraction area between $2\theta = 10°$ and $2\theta = 25°$ and ΣS is the area of all the peaks between $2\theta = 10°$ and $2\theta = 25°$. The values of X_c are listed in Table IV. The X_c values of the samples were in the following order: PP > PP/nCaCO$_3$–5La > PP/nCaCO$_3$–1La > PP/nCaCO$_3$. This result confirmed the aforementioned X_c value calculated by DSC analysis. According to the study by Labour et al.,[27] nCaCO$_3$ as an inorganic filler could improve the nucleation of crystalline PP. After nCaCO$_3$ was covered with a flake of the lanthanum compound, the nucleation was stronger than that of the uncovered

TABLE IV
WAXD Crystalline Parameters of PP and Its Composites

Sample	L_{110} (nm)	L_{040} (nm)	L_{130} (nm)	X_c (%)	f_β (%)
Virgin PP	9.408	8.391	5.821	49.3	0
PP/nCaCO$_3$ (100/10)	11.946	10.071	6.051	44.7	0
PP/nCaCO$_3$–1La (100/10)	10.745	12.573	8.409	46.5	16.9
PP/nCaCO$_3$–5La (100/10)	10.747	12.168	5.821	46.8	21.5

nCaCO$_3$, and the effect of nucleation increased with an increasing concentration of the lanthanum compound; this was the other main reason for nCaCO$_3$–La toughening on PP.

CONCLUSIONS

nCaCO$_3$ was covered by the lanthanum compound by chemical deposition, and the efficacy of this filler for PP was assessed. The notched Izod impact strength increased and then decreased with increasing filler content. The nCaCO$_3$–5La and nCaCO$_3$–1La fillers proved to be effective toughening agents for PP. When the concentration of nCaCO$_3$–5La and nCaCO$_3$–1La reached 15 phr, the maximum notched Izod impact strengths were obtained; they were 300 and 250% of that of virgin PP, respectively. Unlike untreated nCaCO$_3$, transmission electron and scanning electron micrographs showed a uniform size distribution for nCaCO$_3$–La, which dispersed well in PP. After surface modification by the lanthanum compound, the adhesion between the filler particles and PP matrix was enhanced, and aggregation could be avoided. The DSC measurements showed that, in comparison with virgin PP and PP/nCaCO$_3$, the addition of the nCaCO$_3$–La fillers led to a higher crystallization temperature, and nucleation and crystallization were improved at the same time. The WAXD examination revealed that the formation of the β-PP phase was easier with the addition of the lanthanum compound, and it confirmed that the nCaCO$_3$–La-filled PP showed a stronger nucleation ability; these were the main reasons for the toughening effect of nCaCO$_3$–La.

References

1. Liang, J. Z.; Li, R. K. J Appl Polym Sci 2000, 77, 409.
2. Rothon, R. Particulate-Filled Polymer Composites; Wiley: New York, 1995.
3. Reinshagen, J. H.; Dunlap, R. W. J Appl Polym Sci 1976, 20, 9.
4. Kolarik, J.; Jancar, J. Polymer 1992, 33, 4962.
5. Sharma, Y. N.; Patel, R. D.; Dhimmar, I. H.; Bhardwaj, I. S. J Appl Polym Sci 1982, 27, 97.
6. Arellano, M.; Manas, Z. I.; Feke, D. L. Polym Compos 1995, 16, 489.
7. Premphet, K.; Horanont, P. J Appl Polym Sci 1999, 74, 3445.
8. Kazuta, M.; Soji, K.; Hitoshi, K. Polym Eng Sci 1985, 25, 1069.
9. Nakatsuka, T.; Itandani, K. J Colloid Interface Sci 1981, 82, 298.
10. Sharma, Y. N.; Patel, R. D.; Bhardwaj, I. S. J Appl Polym Sci 1982, 27, 97.
11. Jancar, J.; Dibenedetto, A. T.; Dianselmo, A. Polym Eng Sci 1993, 33, 559.
12. Fu, Q.; Wang, G.; Liu, C. Polymer 1998, 36, 2397.
13. Hanprasopwattana, A.; Srinivasan, S.; Sault, A. G.; Datye, A. K. Langmuir 1996, 12, 3173.
14. Aubert, M.; Macaudiere, P. U.S. Pat. 6,221,473 (2001).
15. Yasuda, H.; Tamai, H. Polym Sci 1993, 18, 1097.
16. Wilson, D. J. Polym Sci 1995, 33, 2505.
17. Feng, J. C.; Chen, M. C.; Huang, Z. T. J Appl Polym Sci 2001, 82, 1339.
18. Thio, Y. S.; Argon, A. S.; Cohen, R. E.; Weinberg, M. Polymer 2002, 43, 3661.
19. Maiti, I. N.; Mahapatro, P. K. J Appl Polym Sci 1991, 42, 3101.
20. Chan, C. M.; Wu, J. S.; Li, J. X.; Cheung, Y. K. Polymer 2002, 43, 2981.
21. Tjong, S. C.; Li, R. K. Y.; Cheung, T. Polym Eng Sci 1997, 37, 168.
22. Norton, D. R.; Keller, A. Polymer 1985, 16, 704.
23. Turner, J. A.; Aizlewood, J. M.; Beckett, D. R. Macromol Chem 1964, 75, 134.
24. Tjong, S. C.; Shen, S. J.; Li, R. K. Y. Polym Eng Sci 1996, 36, 100.
25. Tjong, S. C.; Shen, S. J.; Li, R. K. Y. Polymer 1996, 37, 2309.
26. Alexander, L. E. X-Ray Diffraction Methods in Polymer Science; Wiley: New York, 1969; p 423.
27. Labour, T.; Gauthier, C.; Seguela, R.; Vigier, G.; Bomal, Y.; Orang, G. Polymer 2001, 42, 7127.